May 1995

Disorder and Noncollinear Magnetism in Permanent-Magnet Materials with the $ThMn_{12}$ Structure

R. Lorenz
Institut für Theoretische Physik, Technische Universität Wien, Wiedner Hauptstrasse 8-10, A-1040 Wein, Austria

J. Hafner
Institut für Theoretische Physik, Technische Universität Wien, Wiedner Hauptstrasse 8-10, A-1040 Wein, Austria

Sitaram Jaswal
University of Nebraska, sjaswal1@unl.edu

David J. Sellmyer
University of Nebraska-Lincoln, dsellmyer@unl.edu

Disorder and Noncollinear Magnetism in Permanent-Magnet Materials with the $ThMn_{12}$ Structure

R. Lorenz,[1] J. Hafner,[1] S. S. Jaswal,[2] and D. J. Sellmyer[2]

[1]*Institut für Theoretische Physik, Technische Universität Wien, Wiedner Hauptstrasse 8-10, A-1040 Wein, Austria*

[2]*Behlen Laboratory of Physics and Center for Materials Research and Analysis, University of Nebraska, Lincoln, Nebraska 68588-0111*

(Received 28 November 1994)

We report calculations of the noncollinear magnetic structures of $YFe_{12-x}Mo_x$ permanent-magnet materials, using a novel variant of a spin-polarized tight-binding–linear-muffin-tin-orbital technique allowing for local spin-quantization axes on each site and considering spin-orbit coupling. The ternary $YFe_{12-x}Mo_x$ compounds crystallize in the tetragonal $ThMn_{12}$ structure which can be stabilized only by the partial substitution of Fe by an early transition metal like Mo. We show that the substitutional disorder leads to canted spin structures at low Mo content ($x \sim 1$) and to spin-glass-like behavior at higher Mo content ($x \sim 3$).

PACS numbers: 75.25.+z

In recent years the search for improved permanent-magnet materials has been a very active field. A good permanent magnet requires high Curie temperature, large saturation magnetization, and large uniaxial anisotropy. Fe-rich compounds of the type $RFe_{12-x}M_x$ (R = Y, Gd, Nd, Sm; M = Ti, V, Cr, Mo) with the body-centered tetragonal $ThMn_{12}$ structure have a high potential as permanent magnets [1–11]. The addition of the metal M is necessary to stabilize the otherwise unstable RFe_{12} compound. X-ray diffraction [1], neutron diffraction [2], and Mössbauer spectroscopy [7] show that the M atoms substitute preferentially for the $8i$ site of the iron in the $ThMn_{12}$ structure. Recent studies of $YFe_{12-x}Mo_x$ show that the magnetization [8,9] decreases faster than the Mössbauer hyperfine field [8,7] with increasing Mo concentration. This may be due to the spin-glass-like behavior which increases with increasing disorder due to Mo substitutions. Such a phenomenon has been observed for $x = 1$ to 3, but not for $x = 4$ (Refs. [7,8]). It is not clear why the sample with $x = 4$ did not show this behavior. The standard electronic structure calculations with a global spin axis fail to explain the observed rapid decrease in the magnetization with increasing x caused by spin frustration or noncollinear magnetism [8]. Also, since these calculations are isotropic, they do not give any information about the observed changes in the magnetocrystalline anisotropy as a function of x (Refs. [10,11]).

In this paper we present a calculation of the noncollinear spin structure for supercells representing $YFe_{12-x}Mo_x$ compounds with various degrees of disorder on the Fe sites of the $ThMn_{12}$ structure, based on a novel variant of the spin-polarized tight-binding–linear-muffin-tin-orbital (LMTO) method with local spin-quantization axes and including an approximate description of spin-orbit coupling. Our calculations show a considerable improvement over the collinear results when compared to experimental data.

Despite the undisputed success of the local spin-density approximation (LSDA) in describing the itinerant magnetism in metals and alloys, the calculation of noncollinear spin structures remains a challenge. In recent years several attempts have been made to extend standard spin-polarized band-structure codes such as the augmented-sperical-wave (ASW) or the LMTO techniques to allow for different directions of the local magnetic moments [12,13]. However, to date applications of these techniques have been restricted to systems with only a few degrees of freedom, such as helical spin structures or intermetallic compounds with frustrated antiferromagnetic structures. Recently, two of us have proposed a novel approach based on the mapping of the LSDA Hamiltonian onto a real-space tight-binding Hubbard Hamiltonian [14]:

$$H = H_{\text{band}} + H_{\text{exch}} + H_{\text{so}}\,, \tag{1}$$

where H_{band} describes the nonmagnetic part of the band structure, H_{exch} the magnetic exchange splitting, and H_{so} the spin-orbit coupling. The two-center tight-binding Hamiltonian H_{band} is constructed via a canonical transformation from the self-consistent scalar-relativistic LMTO Hamiltonian in the atomic sphere approximation [15]. The formulation of the exchange part is based on the assumption that the local exchange splitting Δ_{il} is proportional to the local spin polarization,

$$\Delta_{il} = I_l \mu_{il}\,, \tag{2}$$

with an effective Stoner parameter I_l for the band with angular quantum number l, leading to

$$H_{\text{exch}} = -\frac{1}{2}\sum_{ilm}\Delta_{il}\sum_{ss'}X^{\vec{\zeta}_i}_{ss'}c^{\dagger}_{ilms}c_{ilms'}\,, \tag{3}$$

where

$$\mathbf{X}_{\vec{\zeta}_i} = \mathbf{D}_{\vec{\zeta}_i}\sigma_z\mathbf{D}^{\dagger}_{\vec{\zeta}_i} \tag{4}$$

 0031-9007/95/74(18)/3688(4)$06.00

is the local Pauli spin matrix $\vec{\sigma}_z$ referring to the local quantization axis $\vec{\zeta}_i$, rotated to a global spin axis (the $\mathbf{D}_{\vec{\zeta}_i}$ are the rotation matrices at the site i, and m and s stand for magnetic and spin quantum numbers). The ansatz (3) for the exchange part of the Hamiltonian is based on the observation that the proportionality (2) holds exactly, with a universal value $I_2 = (0.95 \pm 0.015)$ eV for all $3d$ and $4d$ metals ($l = 2$), if the local exchange splitting Δ_{il} is defined in terms of the difference in the position of the center of gravity of the spin-up and spin-down bands [16] [for a general discussion of the mapping of the LSDA exchange-correlation potential on Hubbard- (or Stoner-)–type models, see, e.g., Anisimov, Zaanen, and Andersen [17]; here we only note that in our case the effective Stoner I_l has to be identified with Hund's rule exchange]. The spin-orbit-coupling term is given by

$$H_{\mathrm{so}} = \sum_i \xi_i \vec{\sigma}_i \cdot \vec{L}_i , \tag{5}$$

where ξ_i is the spin-orbit-coupling matrix element calculated with the self-consistent scalar relativistic wave functions.

The self-consistent spin structure is then calculated using an iterative real-space recursion algorithm. Starting with a random distribution of the local spin-quantization axes $\vec{\zeta}_i$, for each atomic site i the local spin-polarized partial densities of state $n_{ilms}(E)$ for spins parallel and perpendicular to $\vec{\zeta}_i$ are calculated using the recursion method [18]. Integrating the $n_{ilms}(E)$ up to the Fermi level defines the updated local magnetic moment $\vec{\mu}_{ilm}$. In general, $\vec{\mu}_{ilm}$ will have transverse components with respect to $\vec{\zeta}_i$ and the new local quantization axis $\vec{\zeta}_i'$ must be rotated into the direction of the moment. The calculation is iterated until the directions are stabilized and self-consistency according to Eq. (2) has been achieved. The main advantage of this technique is that in essence we calculate the magnetic force that rotates the moment into the direction of easy magnetization. Convergence is usually quite fast, except when an almost collinear configuration is approached. In this case, the force acting on the local moments is very small close to equilibrium and convergence is slowed down. The technique is also very useful in the absence of competing exchange interactions because it immediately predicts the easy axis of magnetization and allows, by repeating the calculation in the presence of a magnetic field perpendicular to the easy axis, to determine the value of the anisotropy constant without calculating very small energy differences [19]. Here we concentrate on the noncollinearity induced by the substitutional disorder, but it is important to include the local anisotropies arising from the spin-orbit coupling in the calculations.

The calculations have been performed for a periodically repeated supercell containing 52 atomic sites (four formula units or two $ThMn_{12}$ unit cells). In a first series, Mo was substituted only on randomly selected $8i$ sites (note that in this case YFe_8Mo_4 is again a fully ordered intermetallic compound). In a second series, for $x = 3$ and $x = 4$ one Mo atom per formula unit was placed on an $8j$ instead of an $8i$ site. The local spin-polarized density of states, local moments, and spin splittings are calculated self-consistently on all 52 sites, using 25 recursion steps for d states and nine recursion steps for s and p states. The results for the absolute values of the local moments (averaged over the crystallographically equivalent sites) and for the average moment per formula unit are given in Table I. If the Mo atoms occupy only the $8i$ sites, we find a reduction of the calculated macroscopic magnetization compared to the collinear case, whereas the absolute values of the local moments are only little affected. This reduction is 12% for $x = 1$, 40% for $x = 2$, and 30% for $x = 3$, whereas for $x = 4$ a collinear configuration is retained as expected. This means that for larger Mo content these calculations do not reproduce the observed reduction of the magnetic moment. If for $x = 3{,}4$ one Mo atom per formula unit is placed on one of the $8j$ sites, the macroscopic magnetization drops dramatically and is now in very good agreement with experiment. That the calculations underestimate the global magnetization for $x = 1$ and $x = 2$ is probably a consequence of the small size of the supercell: In the real alloy, the Mo contents of the unit cells fluctuate so that the strong disorder effects in those with $x = 1$ and $x = 2$ will be averaged out against the absence of disorder in those with $x = 0$ and the weaker disorder in those with $x = 3$, as long as Mo occupies only the $8i$ sites. Occupation of the $8j$ sites occurs only for high global Mo concentrations. It is important to emphasize that, although due to the disorder the global magnetization is strongly re-

TABLE I. Absolute values of average local magnetic moments $|\vec{\mu}_l|$ (in Bohr magnetons) in substitutionally disordered $YFe_{12-x}Mo_x$ alloys and magnetic moment $\bar{\mu}$ per formula unit. (a) Mo atoms are substituted only on the $8i$ sites; (b) Mo atoms are distributed over the $8i$ and $8j$ sites (cf. text). The results given in the lines marked with an asterisk refer to the collinear calculations (Ref. [8]); the results in the lines marked with a double asterisk give the results obtained by Coehoorn (Ref. [3]) in the limiting cases of the ordered compounds.

(a)

			$\vec{\mu}_l$			$\bar{\mu}$	
x	Y(a)	Mo(i)	Fe(i)	Fe(j)	Fe(f)	Theor.	Expt.[a]
0**	−0.39	–	2.32	2.26	1.86	24.1	
1	−0.38	−0.58	2.28	2.09	1.61	18.7	23.7
1*	−0.37	−0.66	2.46	2.11	1.55	21.1	
2	−0.35	−0.43	2.27	1.94	1.55	10.3	14.2
2*	−0.37	−0.53	2.28	2.01	1.62	17.7	
3	−0.30	−0.34	2.04	1.93	1.39	9.5	3.6
3*	−0.32	−0.42	2.03	1.89	1.50	14.0	
4	−0.23	−0.23	–	1.52	1.02	8.9	1.7
4*	−0.27	−0.28	–	1.40	1.23	10.8	
4**	−0.17	−0.21	–	1.34	1.23	8.9	

(b)

			$\vec{\mu}_l$			$\bar{\mu}$	
x	Y(a)	Mo(i,j)	Fe(i)	Fe(j)	Fe(f)	Theor.	Expt.[a]
3	−0.12	−0.27	2.60	2.32	1.16	3.8	3.6
4	−0.16	−0.20	2.15	2.39	1.04	2.8	1.7

[a]Reference [8].

duced, the local magnetic moments are even increased on the $8i$ and $8j$ Fe sites and only slightly reduced on the $8f$ Fe sites. The negative moments carried by the Y and Mo atoms are induced by the strong covalent coupling of the Y and Mo d bands to the minority-spin band of Fe. The Y and Mo local moments are also only weakly affected by the disorder. Hence the reduction of the magnetization results from the disorder in the directions of the local moments.

This is illustrated in Fig. 1 where we show in the left column the distributions of the absolute values $|\vec{\mu}_i|$ of the local moments and in the right column the orientations of the local moments in the form of a vector model. Figure 1(a) refers to the case where Mo atoms substitute only on the $8i$ Fe sites, and Fig. 2(b) to the case where substitution occurs on the $8i$ and $8j$ Fe sites. The mechanism leading to the formation of noncollinear spin structures lies in a competition of ferromagnetic and antiferromagnetic exchange interactions. In the $YFe_{12-x}Mo_x$ compounds, the Fe-Fe nearest-neighbor distances $d_{\text{Fe-Fe}}$ vary between about 2.38 and 2.65 Å. In such a case, the Fe-Fe exchange interactions as a function of distance follow a Slater-Néel curve with a zero close to $d_{\text{Fe-Fe}} \sim 2.45$ Å. It has been pointed out [20] that the existence of strong antiferromagnetic Fe-Fe exchange interactions is important for the height Curie temperatures and large anisotropies of the $YFe_{12-x}M_x$ and the closely related Y_2Fe_{17} compounds. Collinear ferromagnetic ordering is possible only if the antiferromagnetic coupling is locally outbalanced by stronger ferromagnetic interactions. For $YFe_{11}Mo_1$ we find that most moments are concentrated along the z direction; only two Fe($8j$) moments are oriented almost perpendicular to the preferred direction. For $YFe_{10}Mo_2$, the moments fan out in a wide angle, and again we observe in the vector model a preference of some Fe moments for an orientation in a plane perpendicular to the direction of the global magnetization. This is even more pronounced in YFe_9Mo_3 (and Mo on the $8i$ sites only) where the eight Fe($8j$) moments lie in pairs in a plane perpendicular to the other Fe spins which show only a slight canting from the easy axis. This is the classical solution for antiferromagnetic moments in an almost uniform field resulting from the other Fe atoms. YFe_8Mo_4 is again a simple collinear ferromagnet (that our figures still show some canting is an artifact: we start from a completely random spin configuration, and to arrange all spins exactly parallel would require extremely long computer runs). If one Mo atom per formula unit is put on the $8j$ sites, the

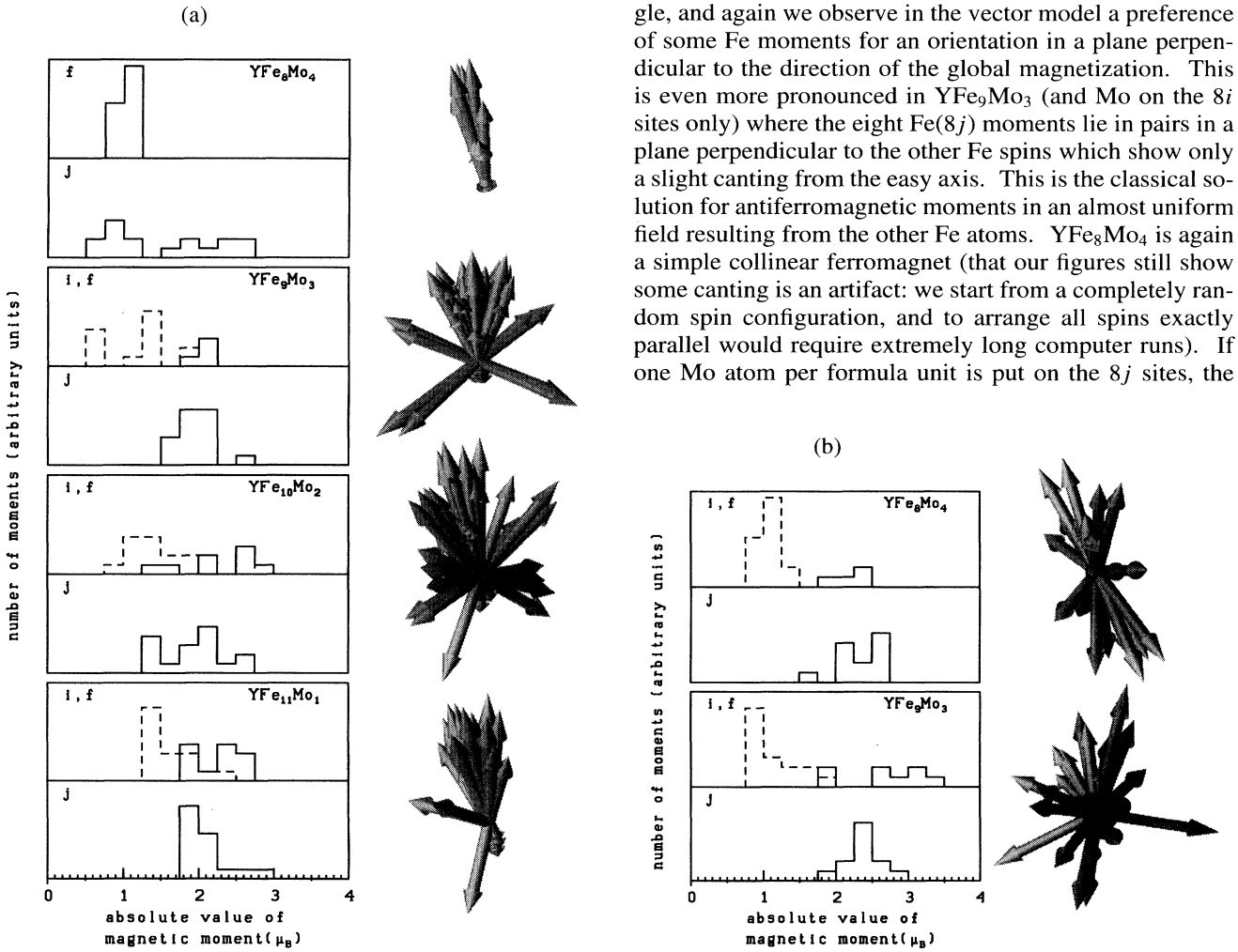

FIG. 1. Distribution of the local magnetic moments in disordered $YFe_{12-x}Mo_x$ alloys. Left column: distribution of the absolute values $|\vec{\mu}_i|$ in the form of a histogram [full line, Fe($8i$) and Fe($8j$); dashed lines, Fe($8f$)]. Right column: Vector model representing the orientations of the local moments. (a) refers to Mo substitution on the Fe($8i$) sites only, and (b) shows the case where one Mo atom per formula unit was placed on an $8j$ site.

character of the spin structure changes [Fig. 1(b)] completely: YFe_9Mo_3 now shows spin-glass-like behavior of the Fe moments, whereas in YFe_8Mo_4 the Fe moments are arranged in a (x, z) plane with a strong antiferromagnetic component in the exchange interactions. Hence the calculations show not only that the substitutional disorder can lead to the formation of noncollinear—in the extreme case almost spin-glass-like—spin structures, but also indicate that the character of the anisotropy changes from uniaxial to planar with higher Mo contents. In principle, the anisotropy can be calculated quantitatively by repeating the calculations in applied fields of varying strength and varying geometry. However, this will require a very high additional computational effort.

In summary, we have performed first-principles self-consistent noncollinear spin-polarized electronic structure calculations for a permanent-magnet material $YFe_{12-x}Mo_x$ with a fairly complex disordered structure, and the results explain reasonably well the observed spin-glass-like behavior and the change in the magnetocrystalline anisotropy as a function of x.

Work at the Technical University Vienna has been supported by the Austrian Ministery for Science and Research under project No. 45.378/2-IV/6/94 ("Magnetism on the nanometer scale") within the framework of the Materials Research Program. Work at the University of Nebraska is supported by the U.S. Department of Energy under Grant No. DE-FG2-86ER45262 and the National Science Foundation under Grants No. INT-91-23488 and No. OSR-925525. The cooperation has been supported within the framework of the Memorandum of Understanding between the National Science Foundation (U.S.) and the Austrian Science Foundation.

[1] D. B. de Mooij and K. H. J. Buschow, J. Less Common Metals **136**, 207 (1988).
[2] Hong Sun, Y. Morii, H. Fujii, M. Akayama, and S. Funahashi, Phys. Rev. B **48**, 13 333 (1993).
[3] R. Coehoorn, Phys. Rev. B **41**, 11 790 (1990).
[4] S. S. Jaswal, Y. G. Ren, and D. J. Sellmyer, J. Appl. Phys. **67**, 4564 (1990).
[5] A. S. Fernando, J. P. Woods, S. S. Jaswal, D. Welipitiya, B. M. Patterson, and D. J. Sellmyer, J. Appl. Phys. **75**, 6303 (1994).
[6] S. Ishida, S. Asano, and S. Fujii, Physica (Amsterdam) **193B**, 66 (1994).
[7] M. Anagnostou, E. Devlin, V. Psycharis, A. Kostikas, and D. Niarchos, J. Magn. Magn. Mater. **131**, 157 (1994).
[8] I. A. Al-Omari, S. S. Jaswal, A. S. Fernando, D. J. Sellmyer, and H. H. Hamdeh, Phys. Rev. B **50**, 4564 (1994).
[9] Hong Sun, M. Akayama, K. Tatami, and H. Fujii, Physica (Amsterdam) **183B**, 33 (1993).
[10] Hong Sun, M. Akayama, and H. Fujii, Phys. Status Solidi (a) **140**, K107 (1993).
[11] Y. Z. Wang, B. P. Hu, L. Song, K. Y. Wang, and G. C. Liu, J. Phys. Condens. Matter **6**, 7085 (1994).
[12] J. Kübler, K. Höck, J. Sticht, and A. R. Williams, J. Phys. F **18**, 469 (1988).
[13] O. N. Mryasov, A. I. Liechtenstein, L. M. Sandratskii, and V. A. Gubanov, J. Phys. Condens. Matter **3**, 7683 (1991).
[14] R. Lorenz and J. Hafner, J. Magn. Magn. Mater. (to be published).
[15] O. Jepsen and O. K. Andersen, Phys. Rev. Lett. **53**, 2571 (1984).
[16] I. Turek, Ch. Becker, and J. Hafner, J. Phys. Condens. Matter **4**, 7257 (1992); Ch. Becker and J. Hafner, Phys. Rev. B **50**, 3933 (1994).
[17] V. I. Anisimov, J. Zaanen, and O. K. Andersen, Phys. Rev. B **44**, 943 (1991).
[18] R. Haydock, V. Heine, and M. J. Kelly, J. Phys. C **8**, 2591 (1975).
[19] R. Lorenz and J. Hafner (to be published).
[20] M. S. Anagnostou, I. Panagiotopoulos, A. Kostikas, D. Niarchos, and G. Zouganelis, J. Magn. Magn. Mater. **130**, 57 (1994).

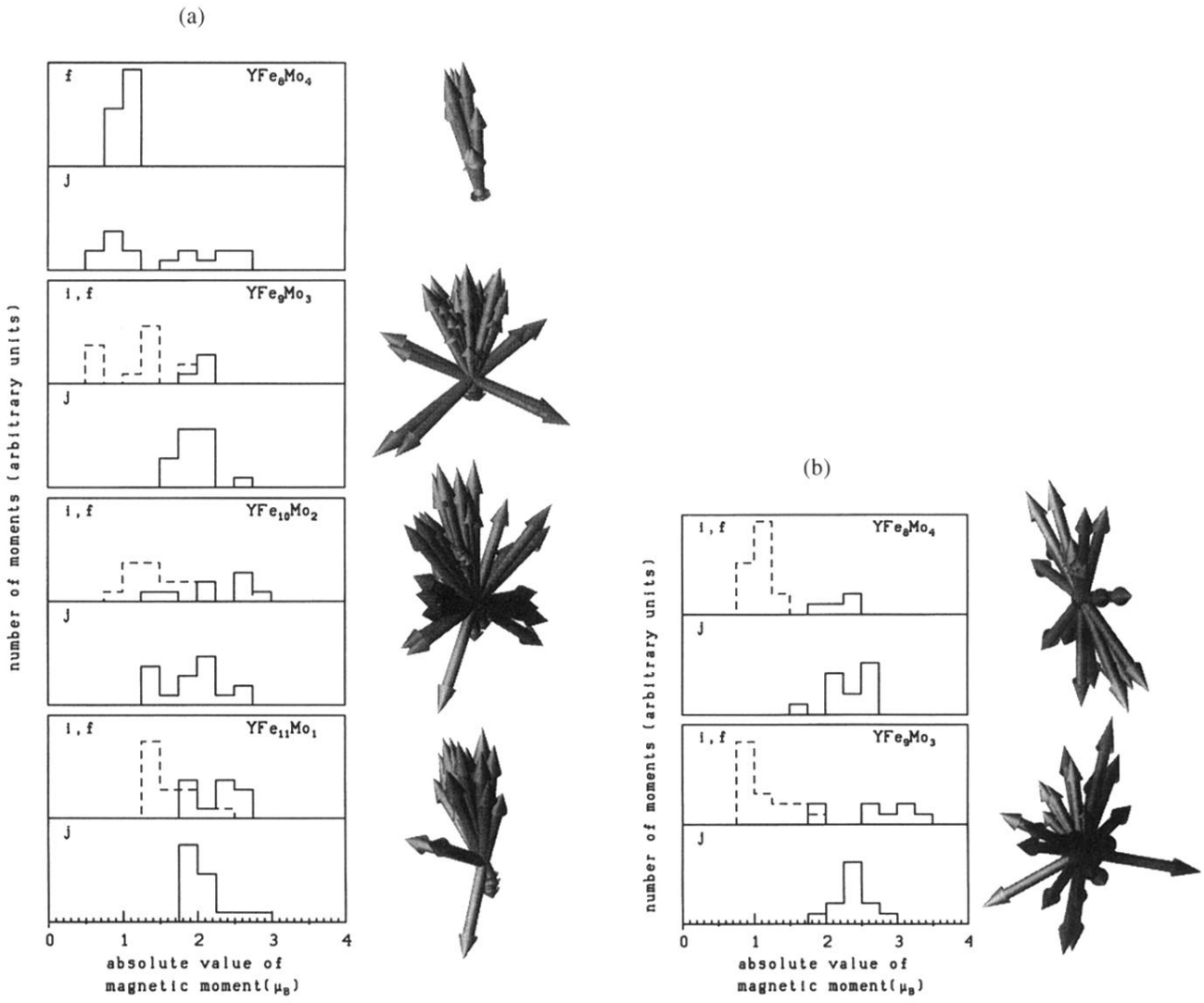

FIG. 1. Distribution of the local magnetic moments in disordered $YFe_{12-x}Mo_x$ alloys. Left column: distribution of the absolute values $|\vec{\mu}_i|$ in the form of a histogram [full line, Fe($8i$) and Fe($8j$); dashed lines, Fe($8f$)]. Right column: Vector model representing the orientations of the local moments. (a) refers to Mo substitution on the Fe($8i$) sites only, and (b) shows the case where one Mo atom per formula unit was placed on an $8j$ site.